Supplemental Table 1. Primer sequences for transcript analysis

Primer		Sequence (5' – 3')	Primer		Sequence (5' – 3')
Mmp2	Forward	ACCCAGATGTGGCCAACTAC	***Mmp15***	Forward	CAGGAAAGGCATGGAACAAT
	Reverse	AAAGCATCATCCACGGTTTC		Reverse	ACCAATGGTGTGACCTGCTC
Mmp3	Forward	TGGAGATGCTCACTTTGACG	***β-Actin***	Forward	CAGCTTCTTTGCAGCTCCTT
	Reverse	AGCCTTGGCTGAGTGGTAGA		Reverse	CACGATGGAGGGGAATACAG
Mmp7	Forward	CGGAGATGCTCACTTTGACA	***Timp1***	Forward	GCATCTGGCATCCTCTTGTT
	Reverse	ACCGGGAACAGAAGAGTGAC		Reverse	TGGGGAACCCATGAATTTAG
Mmp8	Forward	CTTTCAACCAGGCCAAGGTA	***Timp2***	Forward	AAGCAGTGAGCGAGAAGGAG
	Reverse	GAGCAGCCACGAGAAATAGG		Reverse	GGGGGCCGTGTAGATAAACT
Mmp9	Forward	AGACGACATAGACGGCATCC	***Timp3***	Forward	GTGGGAAAGAAGCTGGTGAA
	Reverse	TGGGACACATAGTGGGAGGT		Reverse	AGAGGCTTCCGTGTGAATGT
Mmp10	Forward	CAGTTGGAGAACACGGAGAC	***Col1a1***	Forward	TAAGGGTACCGCTGGAGAAC
	Reverse	TGTCCATTTCTCATCATCATCG		Reverse	CTCCCTGAGCTCCAGCTTCT
Mmp11	Forward	GACGCTGGGAGAAGACAGAC	***Col1a2***	Forward	AGAGGACCACGTGGACAAAG
	Reverse	GTGGGGTCACTTCACTCCATA		Reverse	TGAGCAGCAAAGTTCCCAGT
Mmp12	Forward	GCTGTCACAACAGTGGGAGA	***Fn***	Forward	TTAAGCTCACATGCCAGTGC
	Reverse	ATACCAGATGGGATGCTTGG		Reverse	CCCACTTCTCTCCGATCTTG
Mmp13	Forward	TGGACCTTCTGGTCTTCTGG	***Ccl2***	Forward	AGGTCCCTGTCATGCTTCTG
	Reverse	TGGGCAGCAACAATAAACAA		Reverse	ATTGGGATCATCTTGCTGGT
Mmp14	Forward	CCAGTGGATGGACACAGAGA			
	Reverse	AGAGGGCCGAGAGGTAGTTC			

Abbreviations: *Mmp*, matrix metalloproteinase; *Timp*, tissue inhibitor of metalloproteinase; *Col*, collagen; *Fn*, fibronectin; *Ccl*, chemokine (C-C motif) ligand

Supplemental Figure 1

A

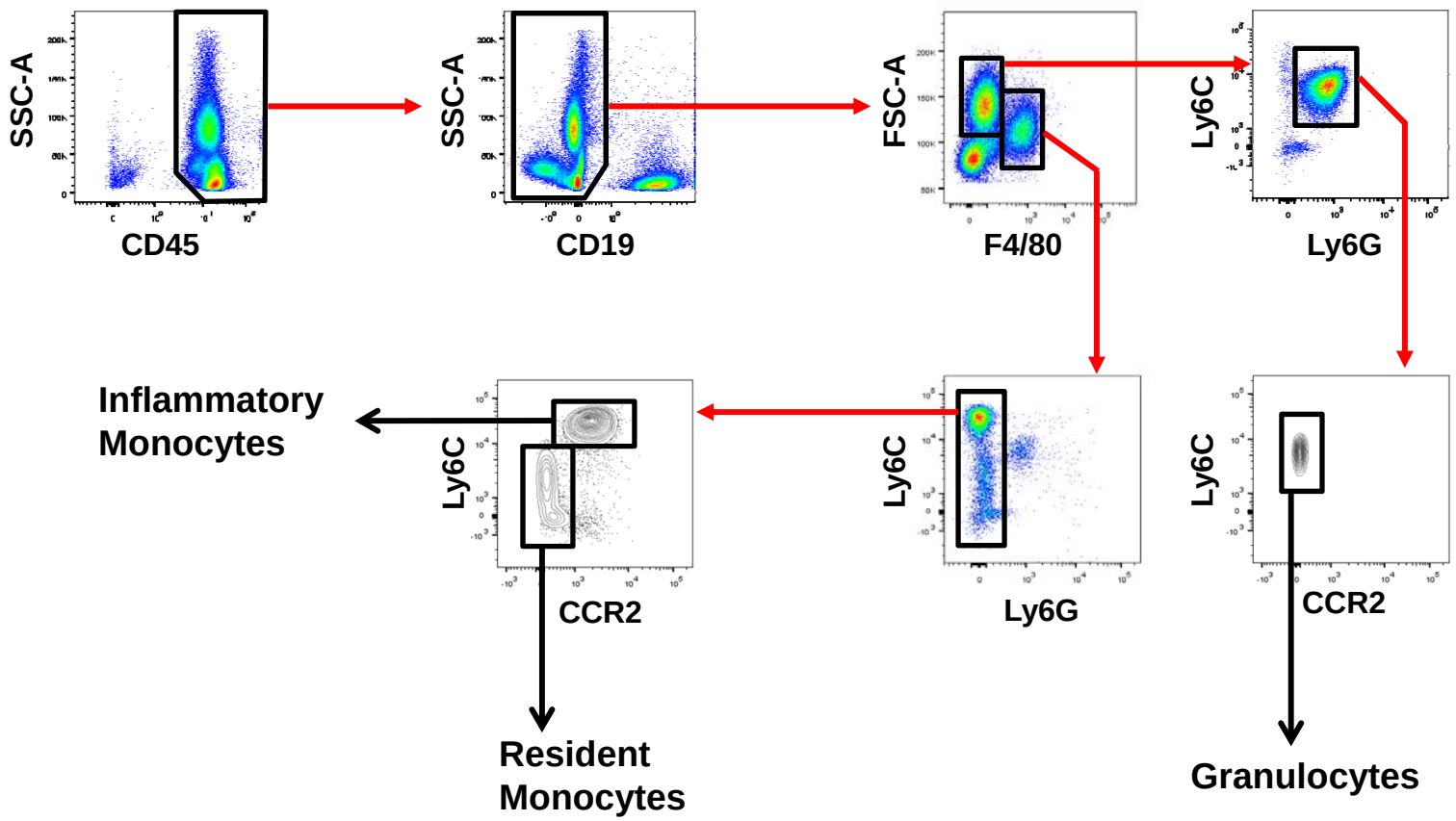

Supplemental Figure 1

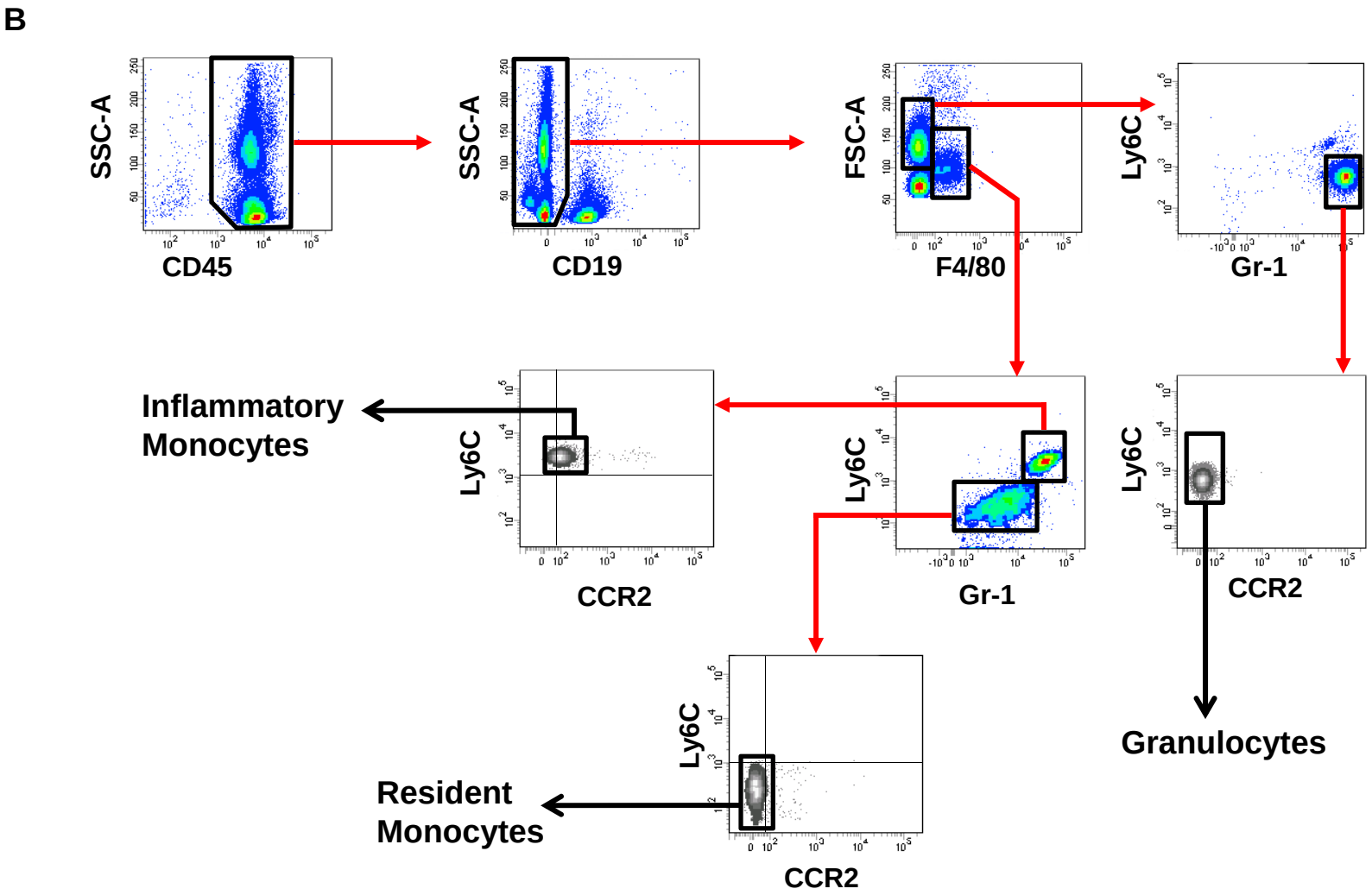

Supplemental Figure 1. Gating strategy for identification of monocyte subpopulations. Fluorescence-activated cell sorting (FACS) plots showing the gating strategy for identifying resident monocytes, inflammatory monocytes and granulocytes using antibodies that recognize (A) Ly6G or (B) Gr-1 in combination with antibodies that recognize CD45, CD19, F4/80, Ly6C and CCR2.

Supplemental Figure 2

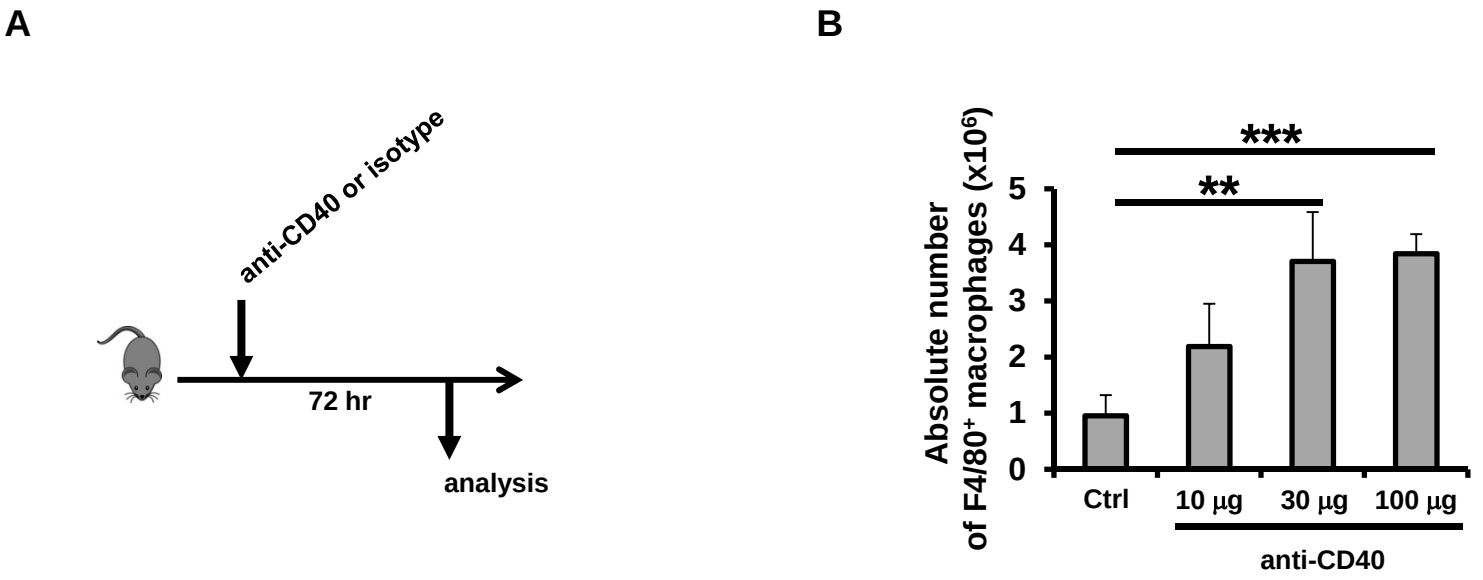

Supplemental Figure 2. CD40 agonist induces accumulation of resident macrophages in spleen. a, Wild-type C57BL/6 mice were administered isotype control or anti-CD40 antibody (0.1 mg) by intraperitoneal injection. **b,** Quantification of the absolute number of F4/80$^+$ macrophages within spleens of mice after treatment with control or escalating doses of anti-CD40. n = 3 mice per group. $^{**}P < 0.01$, $^{***}P < 0.001$, unpaired t-test.

Supplemental Figure 3

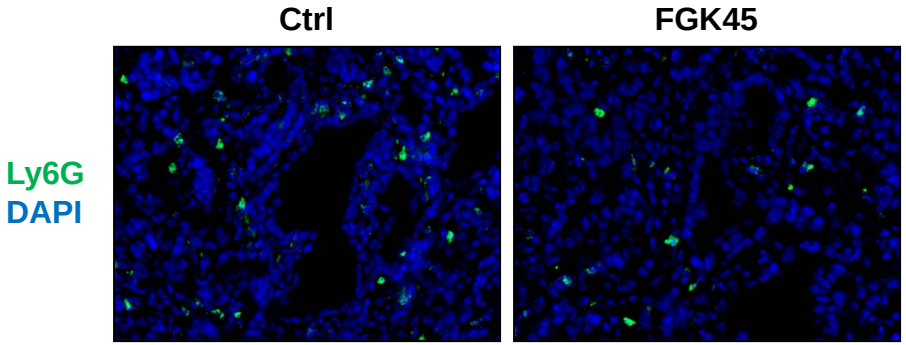

Supplemental Figure 3. Impact of anti-CD40 treatment on Ly6G$^+$ cells within PDAC tumors of KPC mice. Tumor-bearing KPC mice were treated with isotype control (Ctrl) or anti-CD40 antibodies. One day later, tumors were analyzed by immunofluorescence microscopy for the presence of Ly6G$^+$ cells (green). Nuclei are stained with DAPI (blue). Displayed are representative images with quantification shown in **Figure 1H**.

Supplemental Figure 4

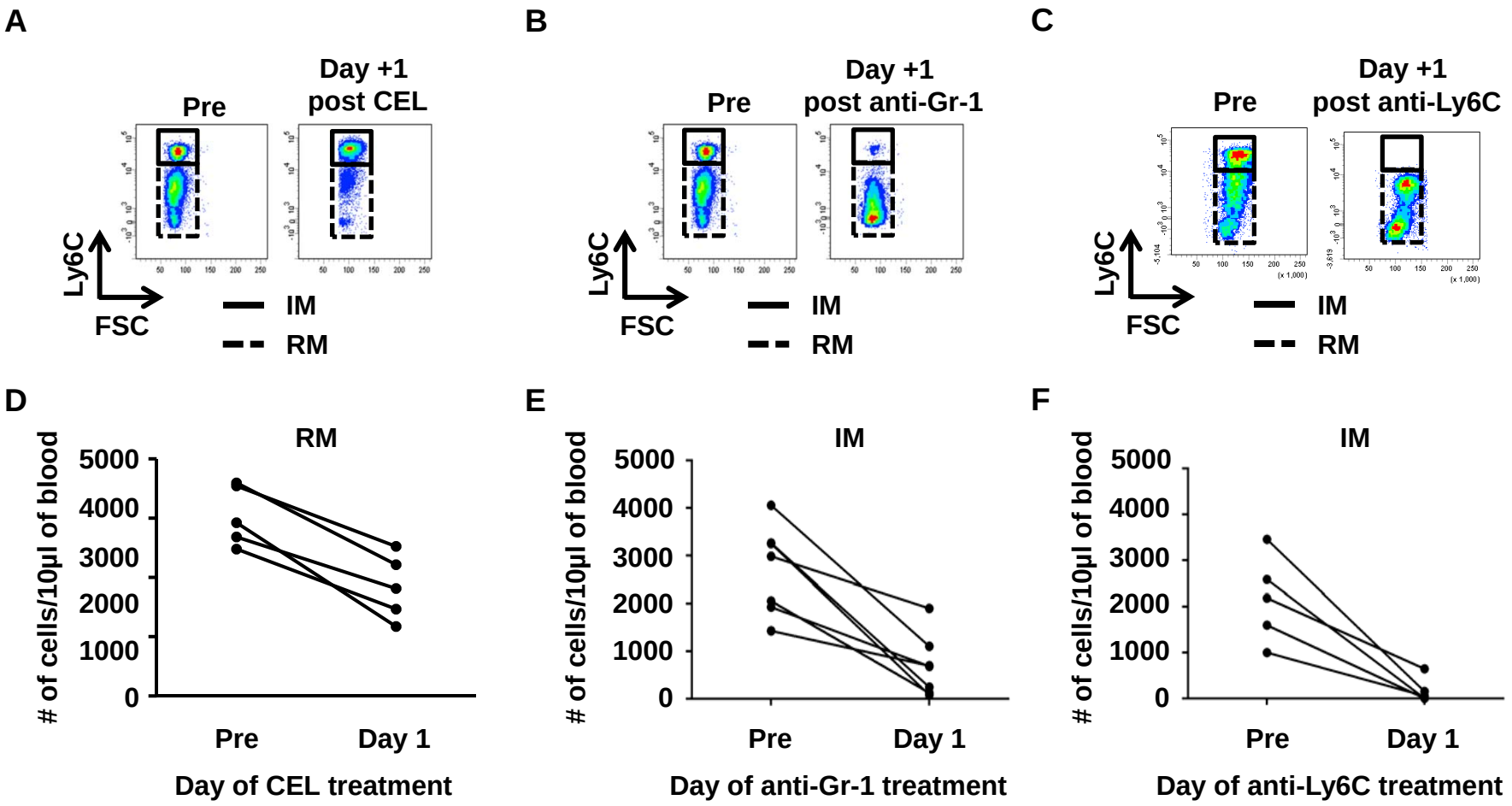

Supplemental Figure 4. Strategy for depletion of resident and inflammatory monocyte populations *in vivo*. FACS plots gated on $CD45^{+}$ $CD19^{neg}$ $F4/80^{+}$ cells showing resident (RM) and inflammatory (IM) monocytes pre and one day post treatment with **a,** clodronate encapsulated liposomes (CEL), **b,** anti-Gr-1 depleting antibody, RB6-8C5, and **c,** anti-Ly6C depleting antibody, Monts-1. **d,** Quantification of absolute number of resident monocytes in peripheral blood pre and post treatment with clodronate encapsulated liposomes. *n*=5 mice, *P* = 0.002, paired *t*-test. **e,** Quantification of absolute number of inflammatory monocytes in peripheral blood pre and post treatment with RB6-8C5 (anti-Gr-1). *n*=7 mice, *P*=0.002, paired *t*-test. **f,** Quantification of inflammatory monocytes in peripheral blood pre and post treatment with Monts-1 (anti-Ly6C). *n*=5 mice, *P*=0.009, paired *t*-test.

Supplemental Figure 5

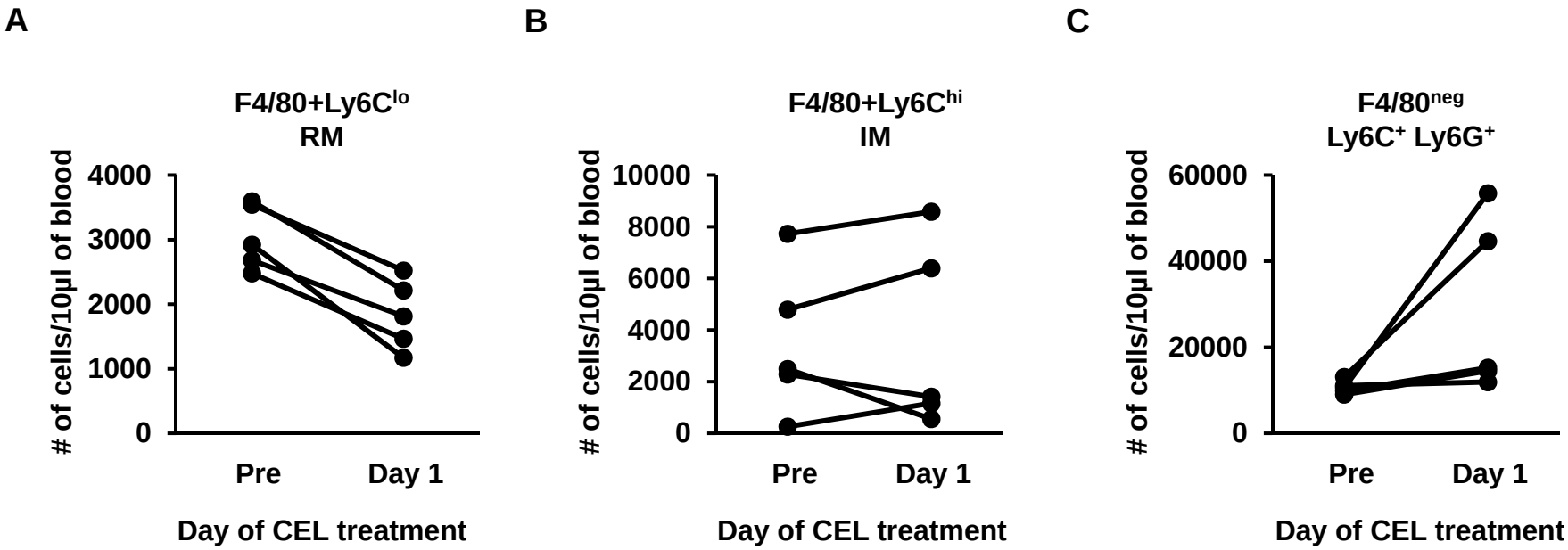

Supplemental Figure 5. Effect of clodronate encapsulated liposome (CEL) treatment on peripheral blood myeloid cells. Shown are peripheral blood counts for **(a)** F4/80^{+} Ly6C^{lo} resident monocytes (RM) , **(b)** F4/80^{+}Ly6C^{hi} inflammatory monocytes (IM) and **(c)** F4/80^{neg} Ly6C^{+} Ly6G^{+} cells prior to (Pre) and one day (Day 1) post treatment with CEL. The impact of CEL on F4/80^{+}Ly6C^{lo} resident monocytes (RM) displayed in **(a)** is also shown in **Supplemental Figure 4D** and depicted here for comparison purposes. Significance testing was performed using a paired *t*-test. *n*=5; F4/80^{+} Ly6C^{lo} RM, *P*= 0.002; F4/80^{+} Ly6C^{hi} IM, *P*= 0.871; F4/80^{neg} Ly6C^{+} Ly6G^{+}, *P* =0.113.

Supplemental Figure 6

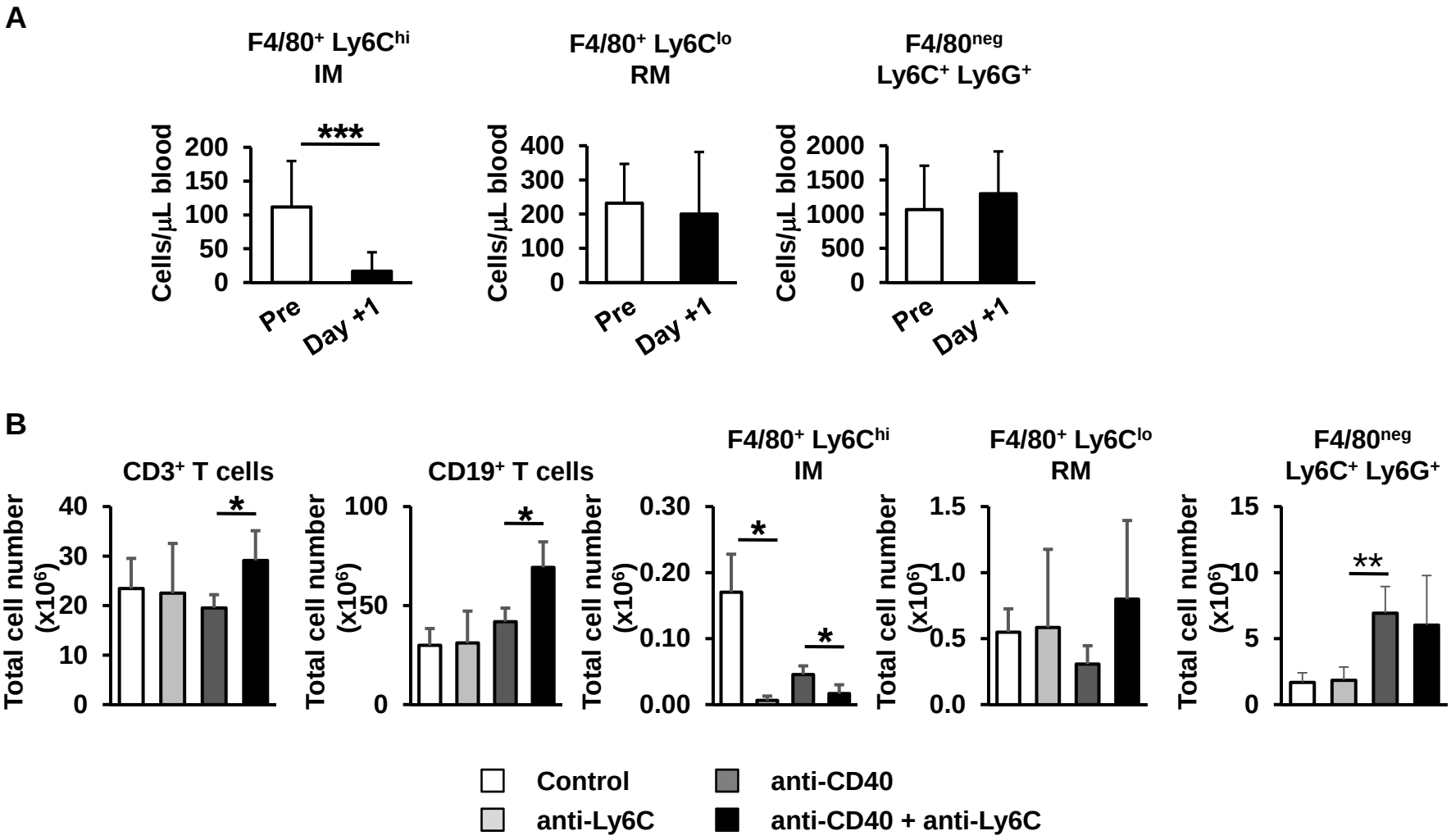

Supplemental Figure 6. Specificity of Ly6C depleting antibody, Monts-1. a, Peripheral blood counts for F4/80^{+} Ly6C^{hi} inflammatory monocytes (IM) , F4/80^{+} Ly6C^{lo} resident monocytes (RM) , and F4/80^{neg} Ly6C^{+} Ly6G^{+} cells prior to (Pre) and one day after (Day +1) treatment with anti-Ly6C depleting antibody, Monts-1. *n*=8 mice, paired *t*-test. **b,** Mice were treated with or without anti-Ly6C on days -1 and 0 with anti-CD40 administered on day 0. Splenocytes were harvested on day +1 and absolute number of CD3^{+} T cells, CD19^{+} B cells, F4/80^{+} Ly6C^{hi} IMs, F4/80^{+} Ly6C^{lo} RMs, and F4/80^{neg} Ly6C^{+} Ly6G^{+} cells were quantified by flow cytometry. *n* = 4 mice/group, 2-tailed unpaired *t*-test. **P*<0.05, ***P*<0.01, ****P*<0.001.

Supplemental Figure 7

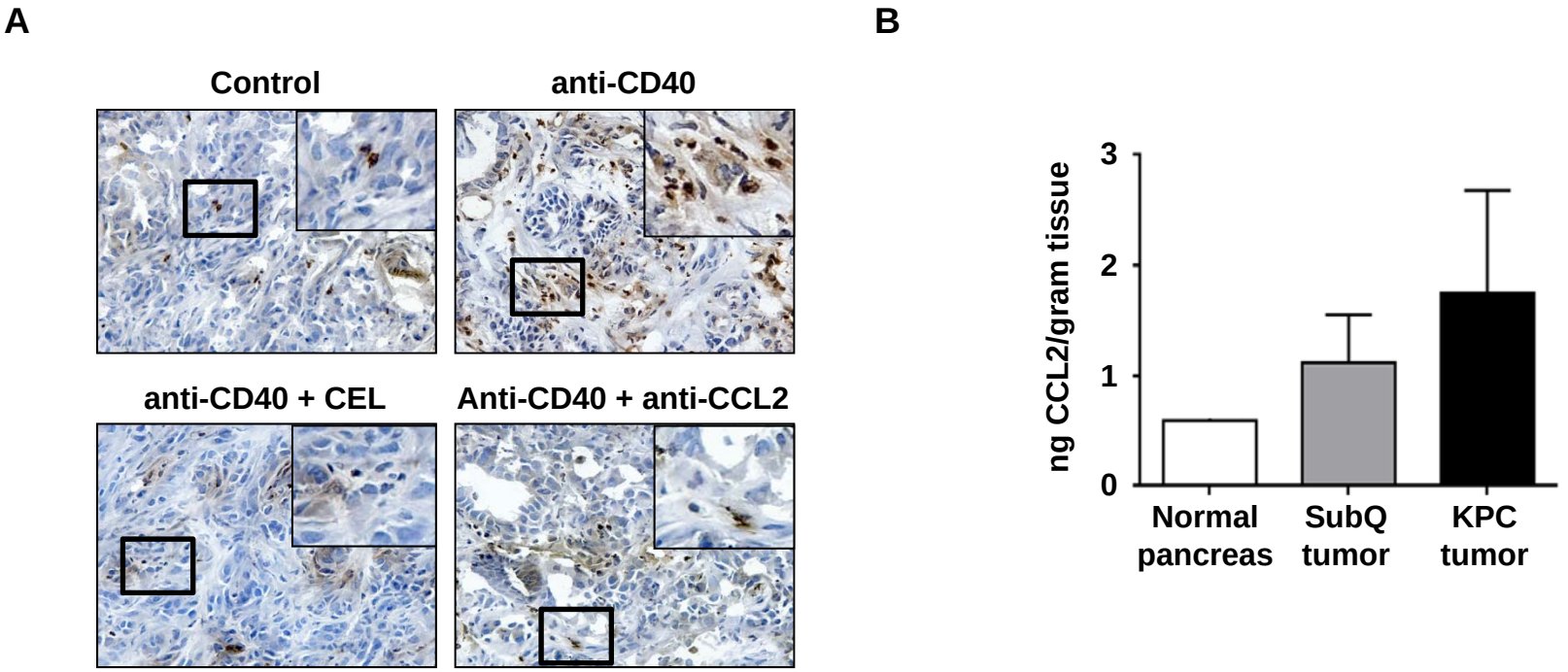

Supplemental Figure 7. CCL2 regulates CD40-dependent Ly6C$^+$ myeloid cell recruitment to PDAC tumors in KPC mice. **a,** Representative images of immunohistochemistry to detect Ly6C$^+$ cells in PDAC tumors from KPC mice one day after treatment with isotype control or anti-CD40 antibodies with or without clodronate encapsulated liposomes (CEL) or anti-CCL2 neutralizing antibodies. Quantification is shown in **Figure 2C**. **b,** CCL2 protein levels detected by cytometric bead array in pancreas of normal littermate (*n*=2), subcutaneously (SubQ) implanted PDAC tumors (*n*=3), and primary PDAC tumors isolated from KPC mice (*n*=4).

Supplemental Figure 8

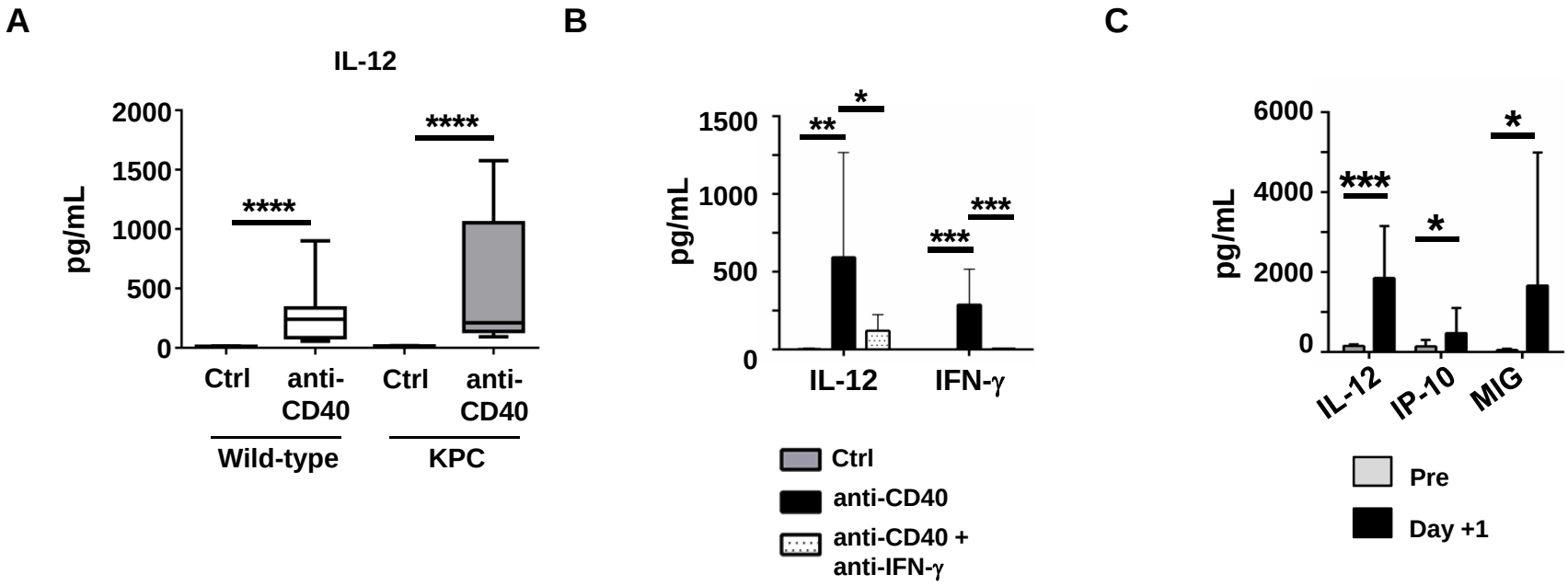

Supplemental Figure 8. Anti-CD40 treatment induces systemic cytokine release in mice and humans. a, Wild-type non-tumor bearing mice and KPC tumor-bearing mice were treated with isotype control (Ctrl) or anti-CD40 antibody. Serum was collected 24 hours after treatment for analysis. Shown are serum levels (pg/mL) of IL-12. *n*=17-20 mice per group for wild-type and *n*=10 mice per group for KPC. **b,** KPC tumor-bearing mice were treated with Ctrl, anti-CD40 or anti-CD40 in combination with anti-IFN-γ neutralizing antibody. Shown are serum levels of IL-12 and IFN-γ detected one day after treatment. *n*=5-14 mice per group. For **a** and **b**, significance testing was performed using Student's 2-tailed unpaired *t*-test. **c,** Shown are plasma levels for IL-12, IP-10, and MIG in PDAC patients Pre and one day post treatment with CP-870,893. For detection of plasma cytokine levels, *n*=13 patients at baseline; *n*=5 patients after CP-870,893. Significance determined using Mann-Whitney test. *, *P*<0.05; **, *P*<0.01; ***, *P*<0.001; ****, *P*<0.0001.

Supplemental Figure 9

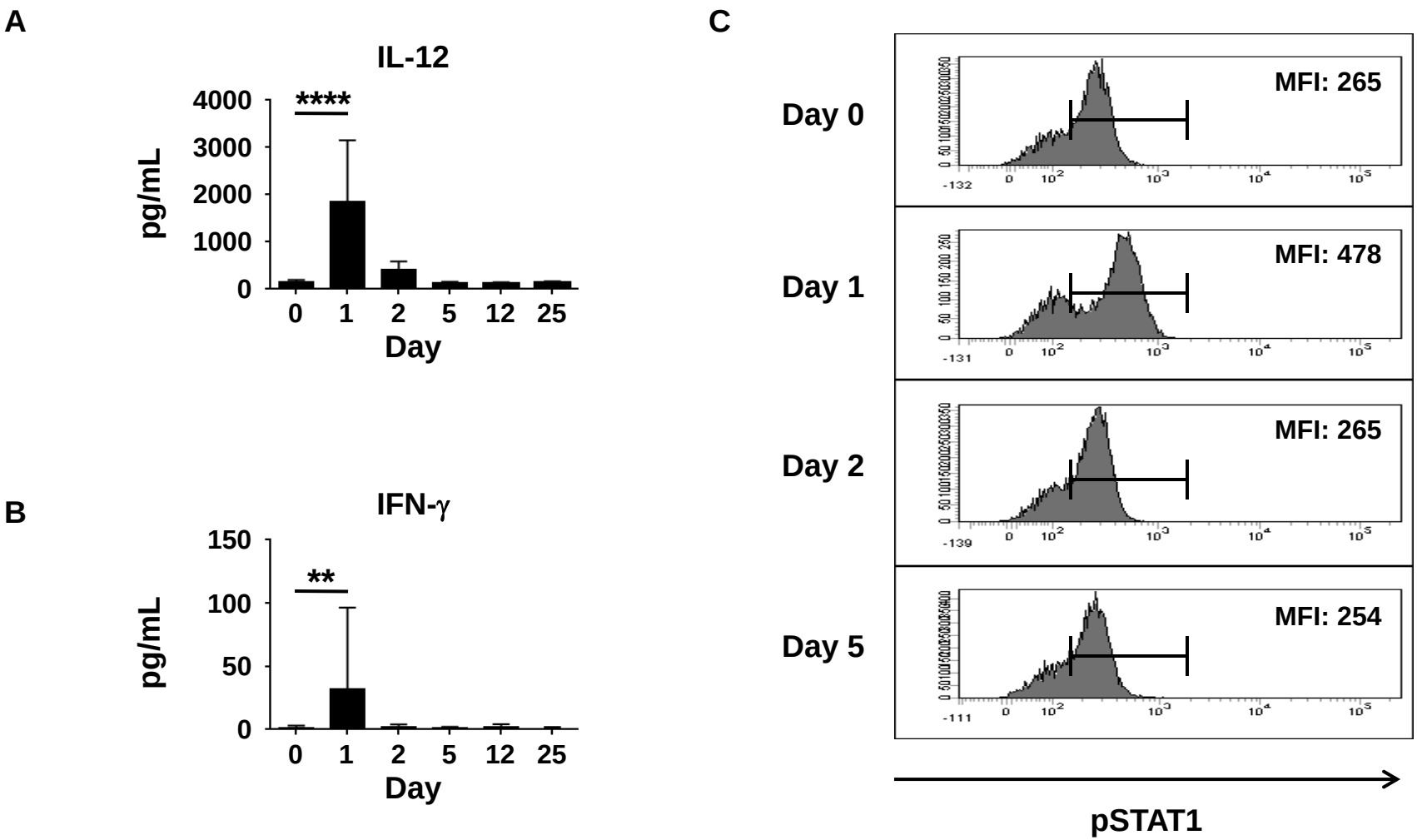

Supplemental Figure 9. STAT1 signaling in human monocytes induced by plasma from PDAC patient treated with CP-870,893. Kinetics of **(a)** IL-12 and **(b)** IFN-γ detected in plasma of PDAC patients prior to and after treatment with the fully human CD40 agonist, CP-870,893. *n*=5-13 patients per time point. **b,** Human monocytes were incubated with plasma collected from a patient at day 0 (prior to treatment) and on days 1, 2, and 5 post treatment with CP-870,893. Monocytes were evaluated by flow cytometry for pSTAT1 expression. Shown are representative histograms of monocytes obtained from one of three healthy volunteers. Quantification of results is shown in **Figure 3D**. MFI, mean fluorescence intensity. For panels **a** and **b**, significance testing was performed using one-way ANOVA with Bonferroni correction. **, $P<0.01$; ****, $P<0.0001$.

Supplemental Figure 10

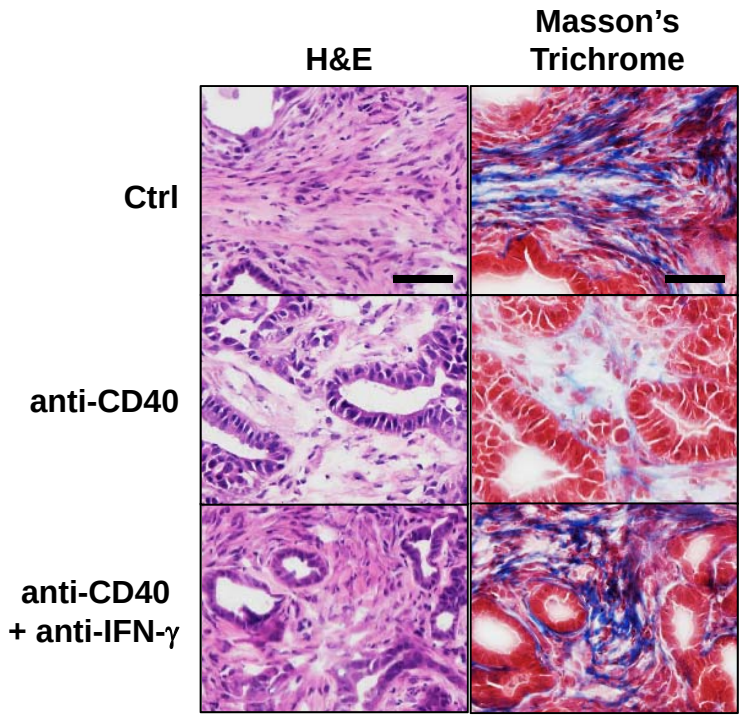

Supplemental Figure 10. Anti-fibrotic activity induced with a CD40 agonist is dependent on IFN-γ. Representative images of tumor sections analyzed by H&E and by Masson's trichrome stain to reveal extracellular matrix (blue) one day after treatment. *n*=5-6 mice per group. Scale bar, 50 μm.

Supplemental Figure 11

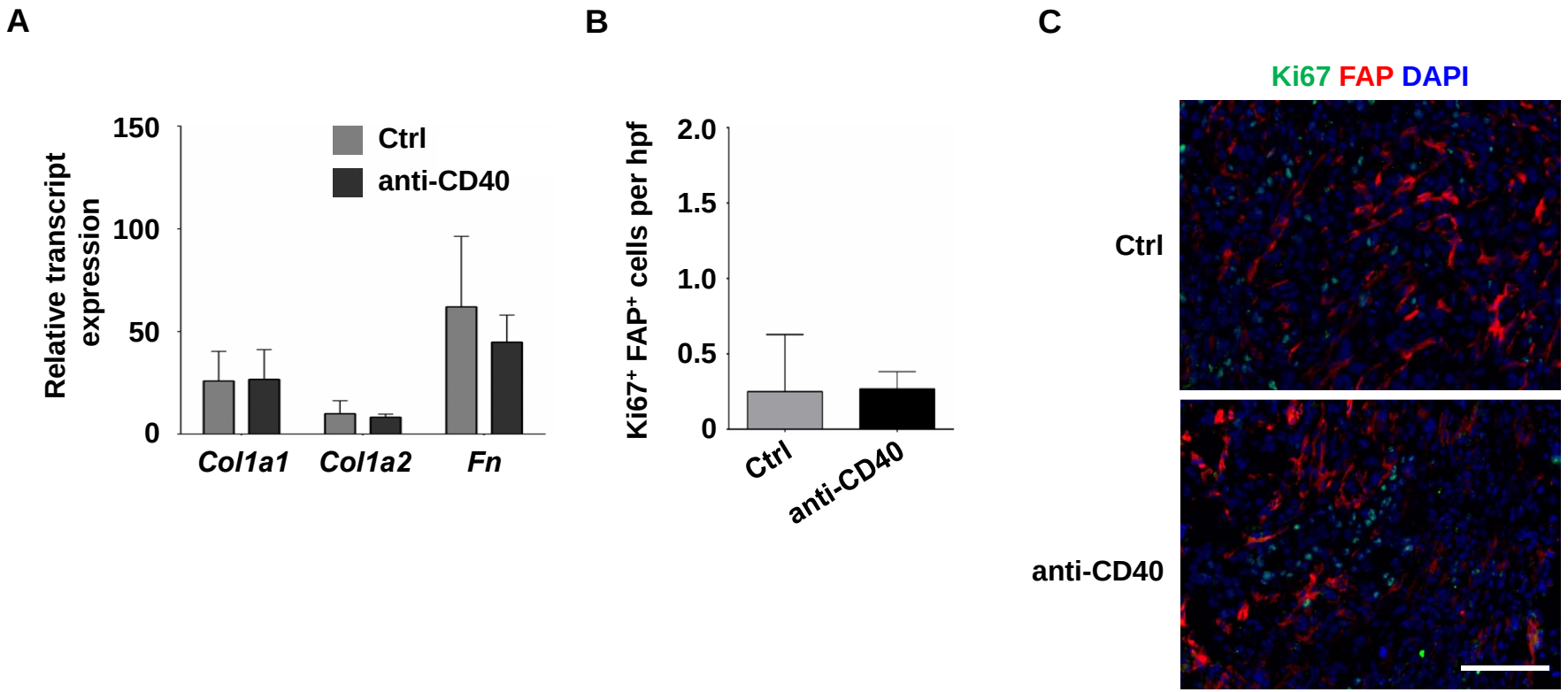

Supplemental Figure 11. CD40 activation does not alter extracellular matrix production or FAP$^+$ fibroblast proliferation. Syngeneic mice bearing established PDAC tumors implanted subcutaneously were treated with isotype control or anti-CD40 antibodies. Tissues were harvested and analyzed one day later. **a,** Shown is relative transcript expression with comparison to *β-actin* for *Col1a1*, *Col1a2*, and *Fn* observed within tumor homogenates. Data are shown as means ± s.d. from *n*=5 mice for each transcript. **b,** Quantification of tumor sections for Ki67$^+$ FAP$^+$ cells by immunofluorescence microscopy. **c,** Representative immunofluorescence images of Ki67 (green) and FAP (red) staining in tumor tissues. Nuclei were stained with DAPI (blue). Scale bar, 100 μm.

Supplemental Figure 12

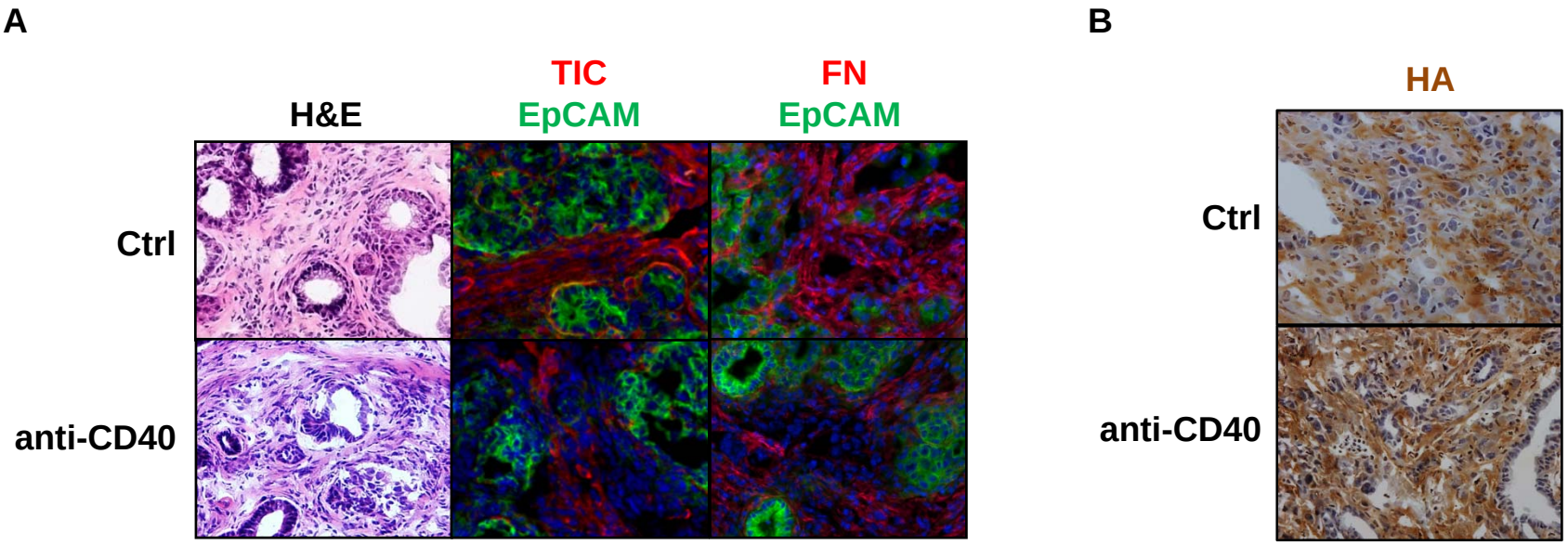

Supplemental Figure 12. Anti-CD40 treatment selectively depletes extracellular matrix proteins within the tumor microenvironment. a, Representative images of H&E and immunofluorescence for type I collagen (TIC) and fibronectin (FN) deposition (red) among $EpCAM^{+}$ tumor cells (green) one day after treatment with isotype control (Ctrl) or anti-CD40 antibodies. **b,** Representative images of immunohistochemistry for hyaluronan (HA) one day after treatment with isotype control (Ctrl) or anti-CD40 antibodies.

Supplemental Figure 13

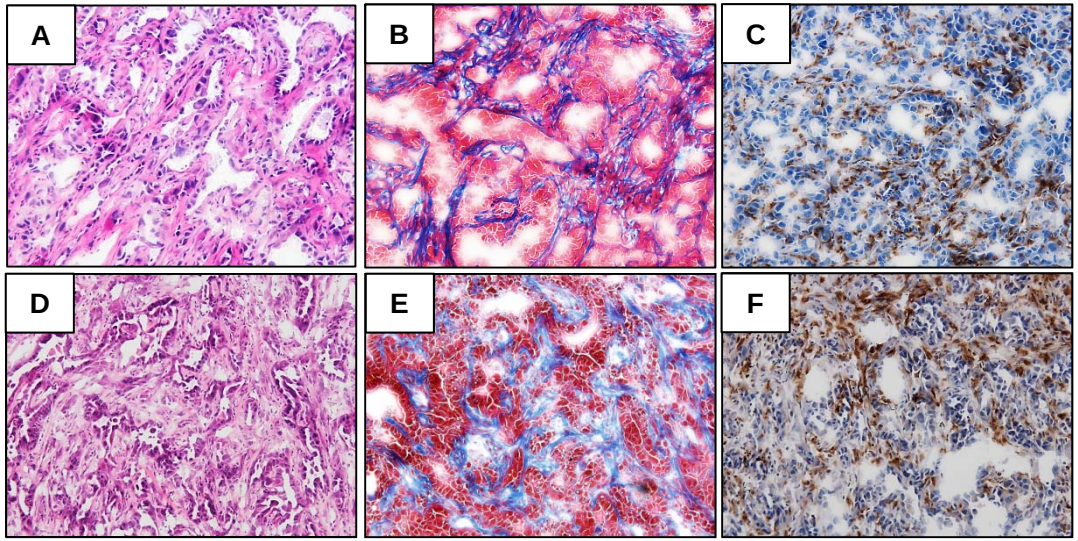

Supplemental Figure 13. Implantable tumor model of PDAC that reproduces tumor microenvironment of KPC model of spontaneous PDAC. Representative images of H&E (A, D), Masson's trichrome staining (B, E) and immunohistochemistry for F4/80^{+} macrophages (C, F) are shown for a spontaneously arising PDAC tumor in the KPC model (A-C) and a cell line derived from this tumor that was implanted subcutaneously into C57BL/6 syngeneic mice (D-F).

Supplemental Figure 14

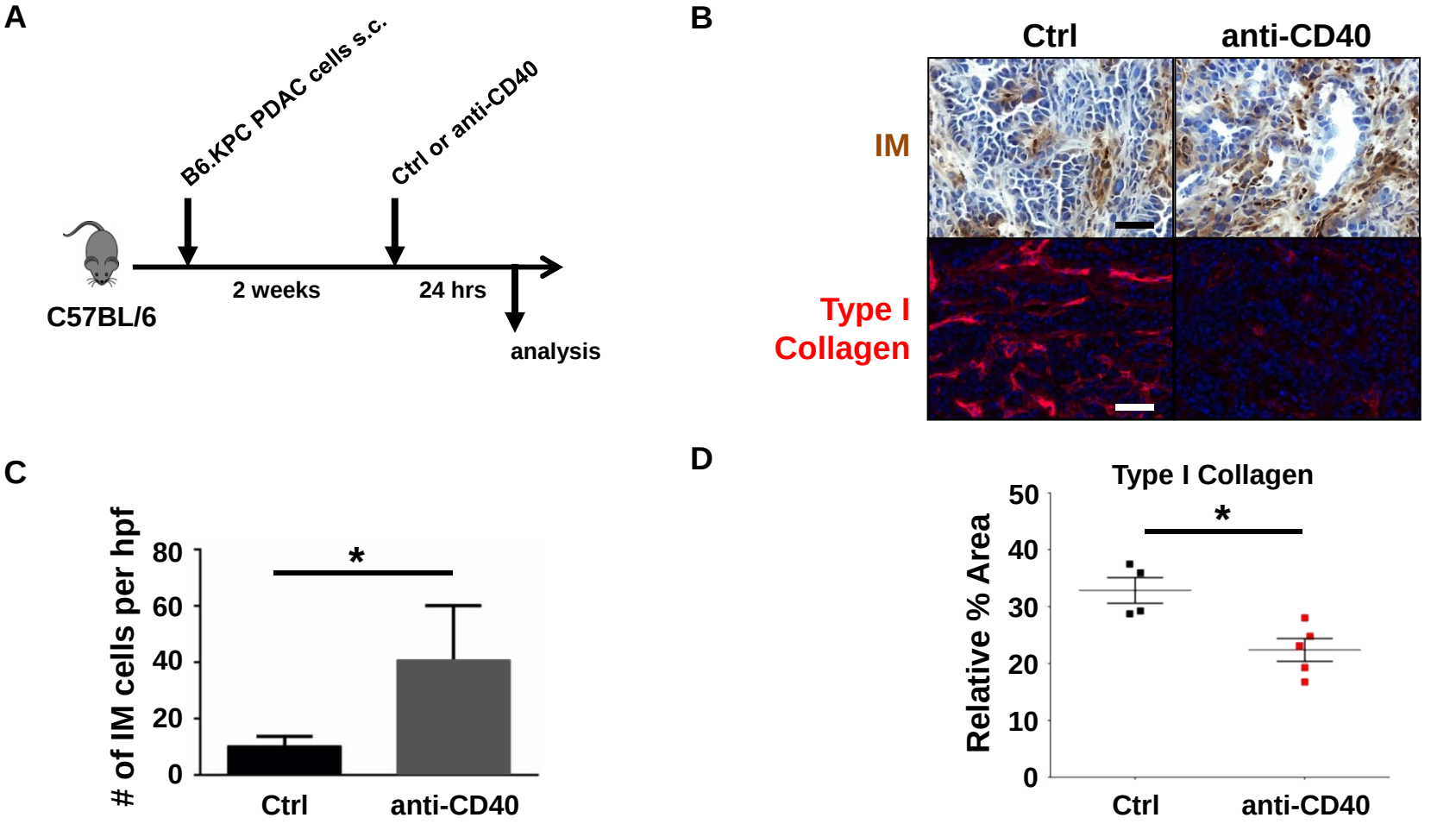

Supplemental Figure 14. Development of an implantable model of PDAC for evaluating monocyte-dependent degradation of cancer fibrosis. a, Schematic showing treatment of C57BL/6 mice implanted subcutaneously with a syngeneic PDAC cell line derived from KPC mice. At two weeks after tumor implantation, mice were treated with isotype control or anti-CD40. The impact of treatment on the tumor microenvironment was examined 24 hours later. **b,** Tumors were analyzed for $Ly6C^+$ inflammatory monocyte (IM) infiltration by staining for Ly6C and for changes in extracellular matrix deposition by staining for type I collagen. One representative image out of 4 is shown per group. Scale bar, 50 μm. **c,** Quantification of tumor-infiltrating $Ly6C^+$ inflammatory monocytes by immunohistochemistry. *, $P < 0.05$; unpaired 2-tailed *t*-test determined from 5-6 images per mouse. **d,** Quantification of type I collagen content. *, $P < 0.05$; unpaired 2-tailed *t*-test determined from 4 images per mouse, n=4-5 mice per group.

Supplemental Figure 15

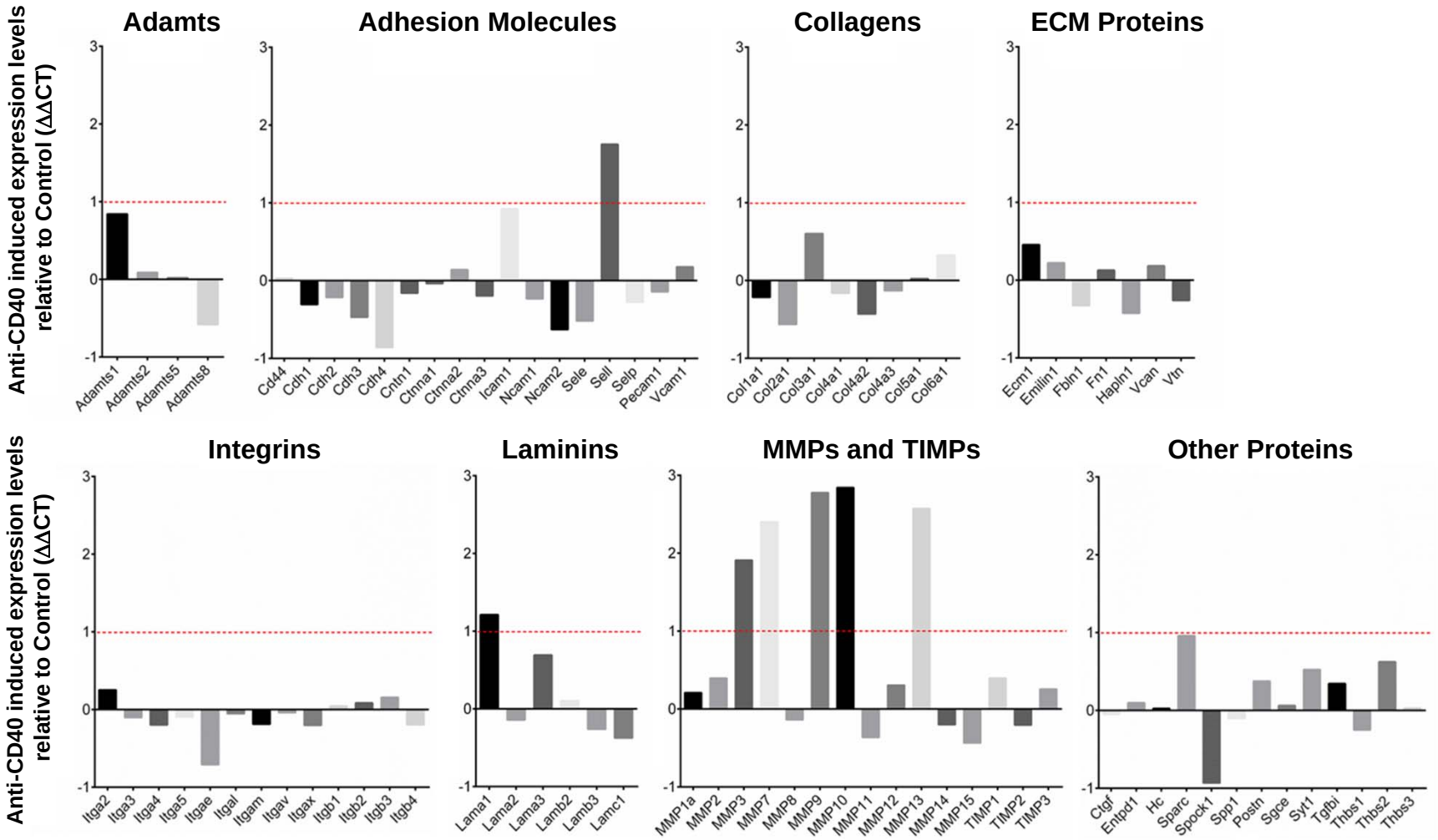

Supplemental Figure 15. Gene expression of extracellular matrix and adhesion molecules within the tumor microenvironment in response to anti-CD40 treatment. Fold change in gene expression within tumor homogenates one day after treatment with anti-CD40 antibodies compared to isotype control.

Supplemental Figure 16

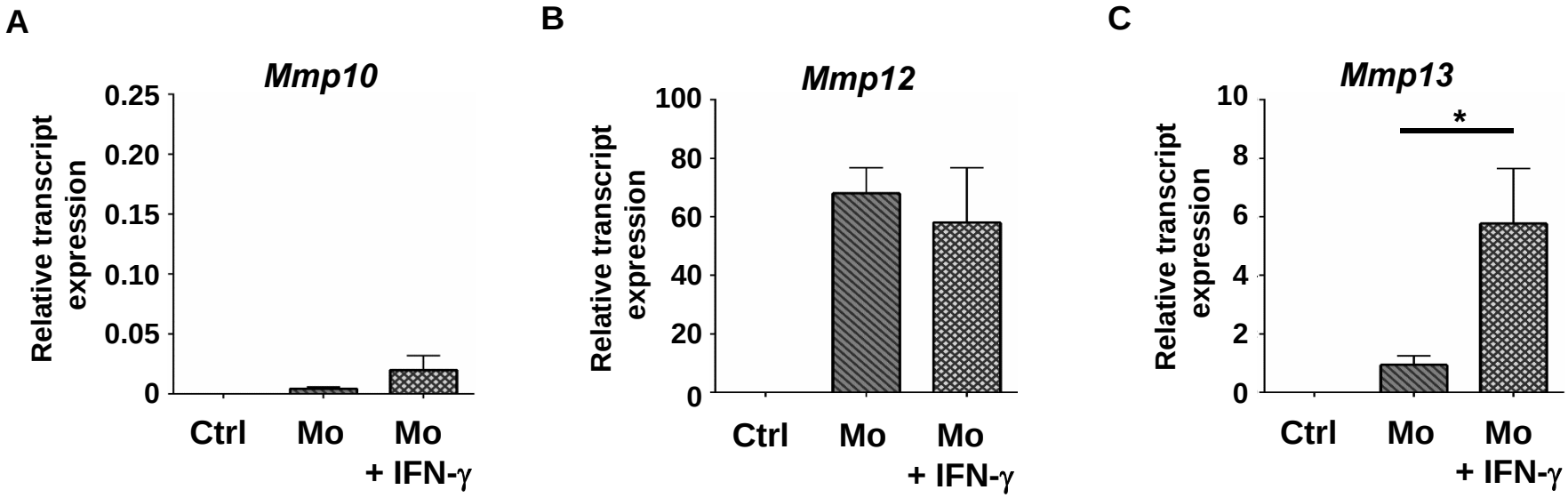

Supplemental Figure 16. IFN-γ induces *Mmp13* expression in myeloid cells. Murine bone marrow derived myeloid cells were stimulated *in vitro* with or without IFN-γ and then plated on a matrix of type I collagen containing human PDAC cells. Murine-specific *Mmp* gene expression was detected 24 hours after addition of unstimulated myeloid cells (Mo), IFN-γ stimulated myeloid cells (Mo + IFN-γ), and no addition of myeloid cells (Ctrl). Shown is the relative transcript expression for **(a)** *Mmp10*, **(b)** *Mmp12*, and **(c)** *Mmp13*. Data are shown as means ± s.d., from 3 independent experiments. *, $P<0.05$.

Supplemental Figure 17

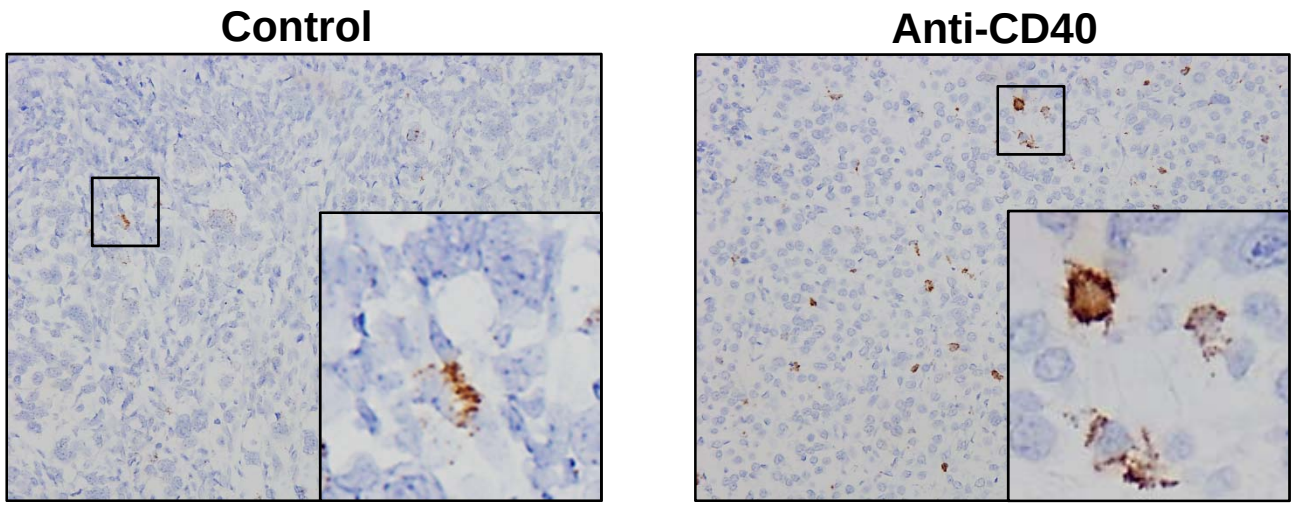

Supplemental Figure 17. RNA *in situ* hybridization (ISH) for MMP13 in PDAC tumors. Representative images of RNA ISH for *Mmp13* in spontaneously arising PDAC tumors in KPC mice one day after treatment with isotype control or anti-CD40 antibody. *n*=3 mice per group, 5 images per mouse.

Supplemental Figure 18

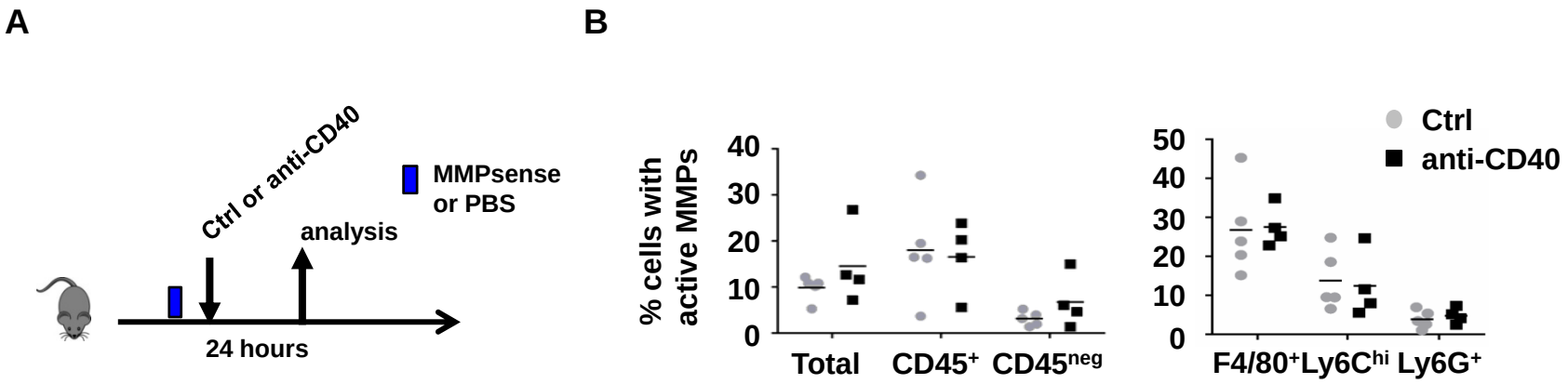

Supplemental Figure 18. Detection of MMP activity in cellular subsets within the tumor microenvironment. Treatment schema for detection of MMP activity. **a,** C57BL/6 mice were injected subcutaneously with PDAC tumor cells and 14 days later mice were administered MMPsense or PBS at three hours prior to treatment with Ctrl or anti-CD40. At 24 hours later, tumors were evaluated by flow cytometry for presence of active MMPs. **b,** Flow cytometric analysis comparing cellular subsets within tumor tissue for the presence of MMP activity. *n* = 4-5 mice per group.

Supplemental Figure 19

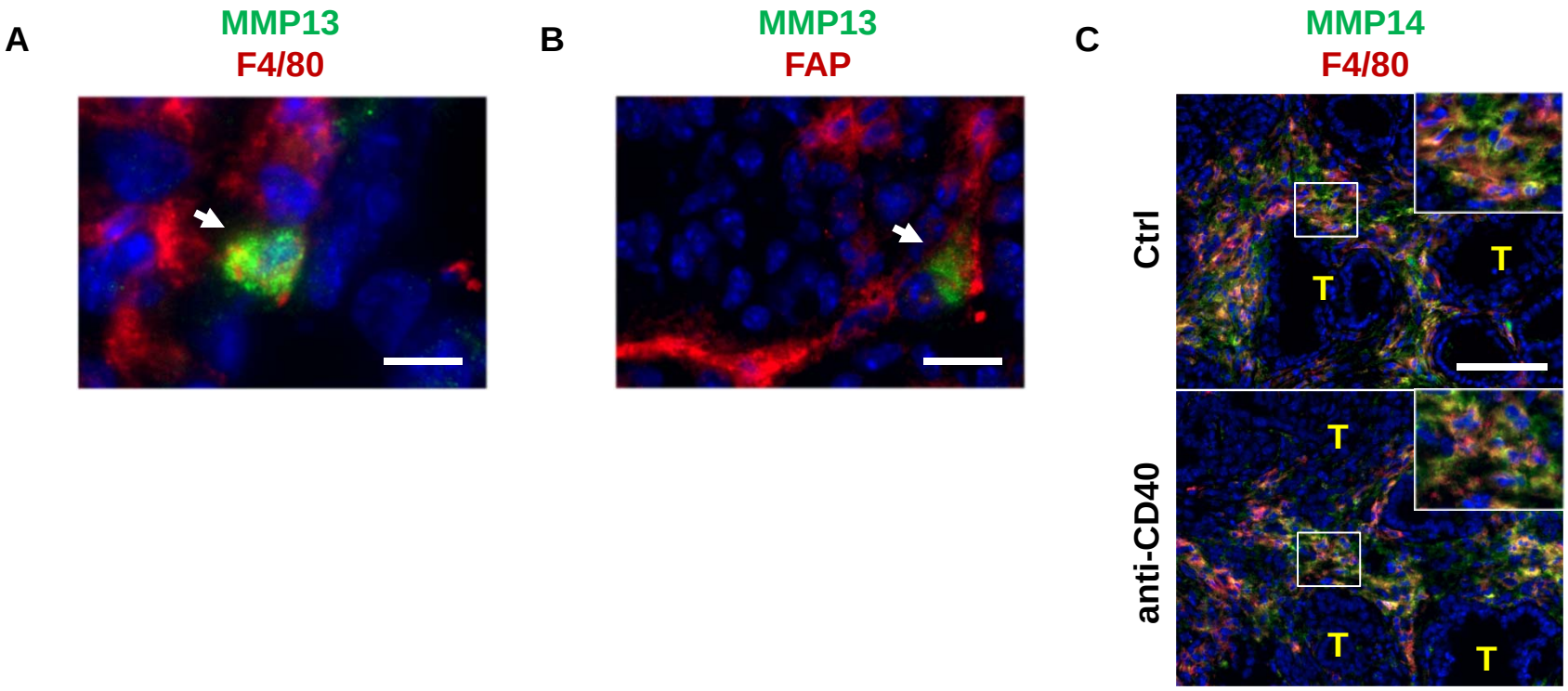

Supplemental Figure 19. Protein expression of MMP13 and MMP14 within the tumor microenvironment of spontaneously arising pancreatic tumors in the KPC model. Representative immunofluorescence images with arrows indicating **a,** MMP13 (green) co-localization with F4/80^{+} (red) myeloid cells (scale bar, 10 μm) and **b,** MMP13 (green) co-localization with FAP^{+} (red) fibroblasts (scale bar, 20 μm) **c,** Expression of MMP14 (green) by F4/80^{+} (red) myeloid cells within stroma but not in tumor cells (T) of KPC mice one day after treatment with isotype control (Ctrl) or anti-CD40 antibody.

Supplemental Figure 20

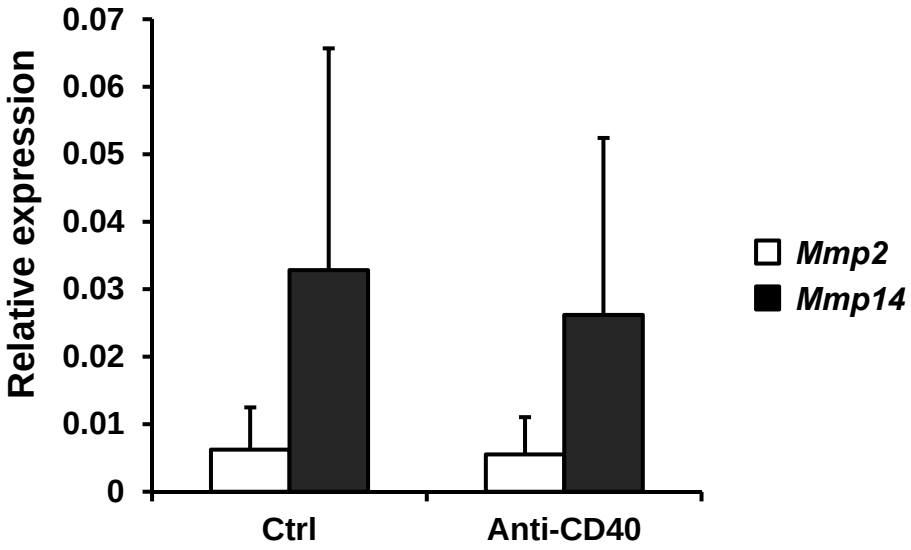

Supplemental Figure 20. Gene expression of *Mmp2* and *Mmp14* within the tumor microenvironment of pancreatic tumors. Shown is the relative transcript expression with comparison to *β-actin* for *Mmp2* and *Mmp14* observed within tumor homogenates one day after treatment (Ctrl versus anti-CD40) of syngeneic mice bearing established PDAC tumors implanted subcutaneously. Data are shown as means ± s.d., from n = 9-10 mice for each transcript.

Supplemental Figure 21

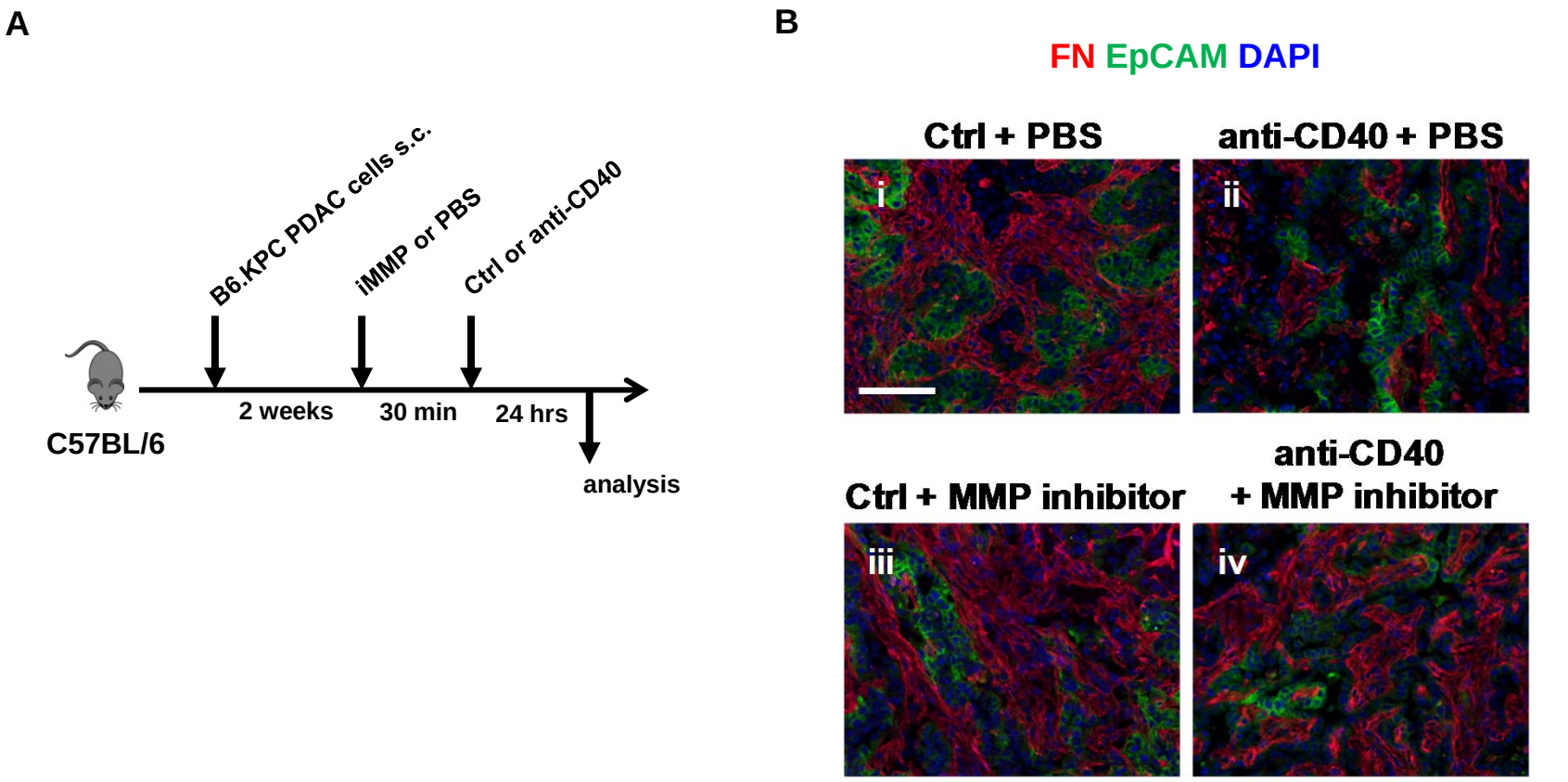

Supplemental Figure 21. Anti-fibrotic activity of a CD40 agonist is dependent on MMPs. a, Schematic showing treatment of mice implanted subcutaneously with a syngeneic PDAC cell line derived from KPC mice. At two weeks after tumor implantation, mice were treated with a broad spectrum MMP inhibitor (iMMP, Actinonin) or PBS followed 30 minutes later by isotype control or anti-CD40 antibodies. **b,** Representative immunofluorescence images show fibronectin (FN, red) deposition among $EpCAM^{+}$ tumor cells (green) one day after treatment. Nuclei are stained with DAPI (blue). One representative image is shown out of five images per tumor section, per group. Scale bar, 100 μm.

Supplemental Figure 22

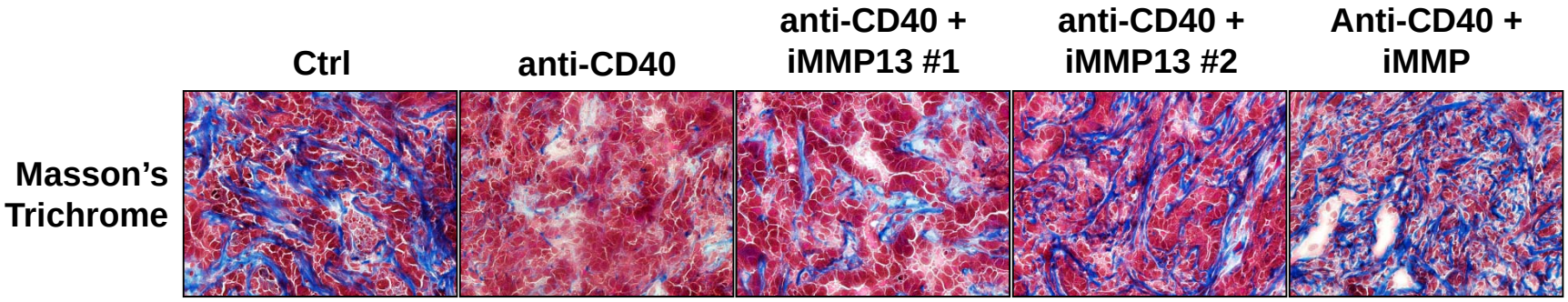

Supplemental Figure 22. Impact of MMP13 specific inhibitors on CD40 agonist induced collagen degradation. Mice with an implanted PDAC tumor were treated with isotype control or anti-CD40 antibodies with or without selective inhibitors of MMP13 (iMMP13 #1, WAY-170523; iMMP13 #2, 544678-85-5) or a broad spectrum MMP inhibitor (iMMP, Actinonin). Representative images show collagen deposition (blue) by Masson's Trichrome staining one day after treatment. One representative image is shown out of five images per tumor section, *n*=4-8 tumors per group.

Supplemental Figure 23

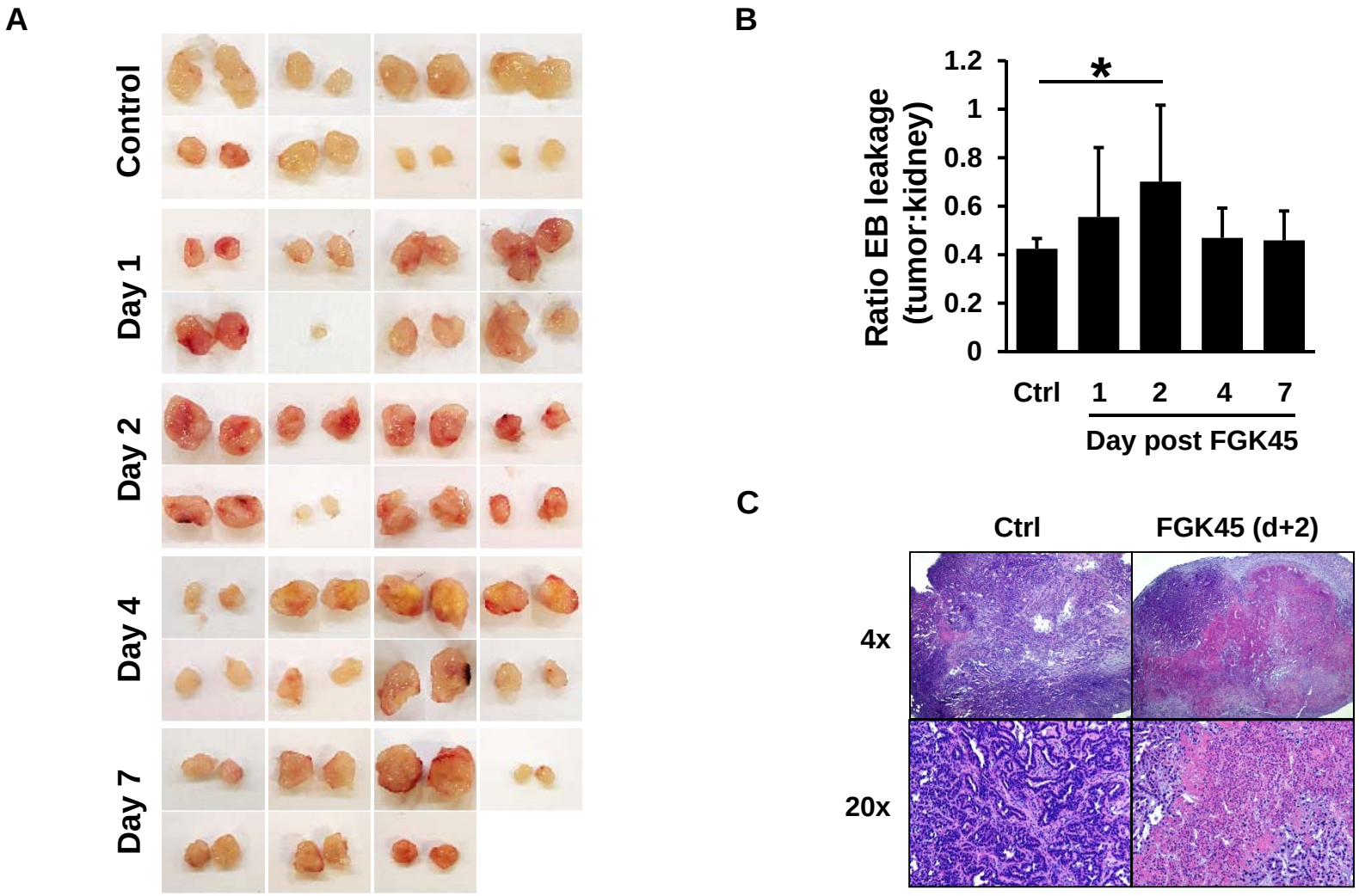

Supplemental Figure 23. Kinetics of anti-CD40 activity on tumor microenvironment. Mice with implanted tumors were analyzed at defined time points after treatment with isotype control or anti-CD40 antibodies. **a,** Gross images of bisected tumors analyzed at indicated time points after anti-CD40 treatment with comparison to isotype control. **b,** Shown is the ratio of Evans Blue (EB) leakage into tumor tissue normalized to kidney. Evans blue was administered 20 minutes prior to necropsy at defined time points after treatment with anti-CD40 or isotype control antibody. **c,** Representative H&E images (4x and 20x) showing hemorrhagic necrosis in tumors at day 2 after anti-CD40 treatment compared to isotype control. n=7-8 tumors per treatment group, *, P<0.05.

Supplemental Figure 24

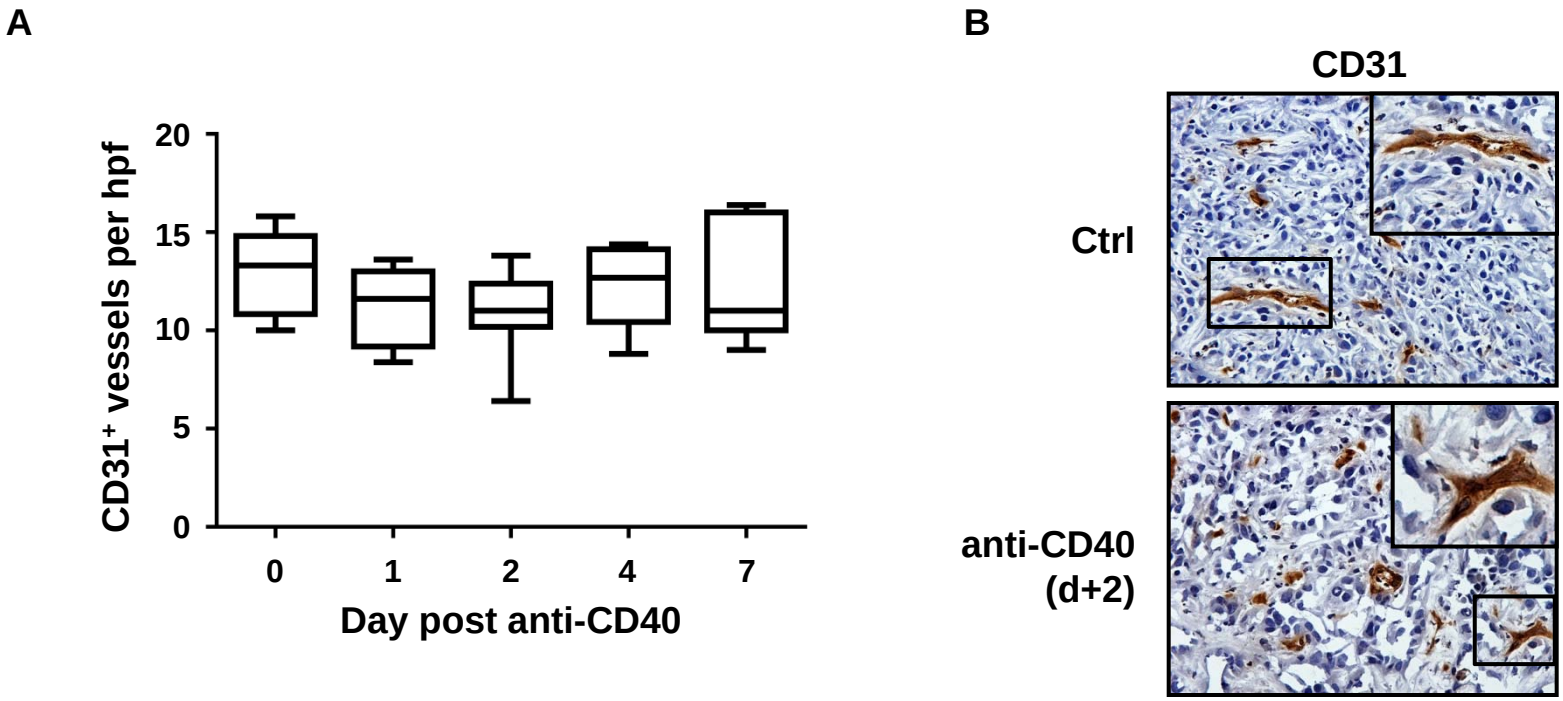

Supplemental Figure 24. Impact of anti-CD40 on CD31⁺ blood vessel density and vascular patency. Mice with implanted tumors were analyzed on multiple days after treatment with isotype control or anti-CD40 antibodies. **a,** Shown is the density of CD31⁺ vessels per hpf. *n*=7-8 tumors per group, 5 images per tumor. **b,** Representative images showing collapsed CD31⁺ blood vessels within tumors.

Supplemental Figure 25

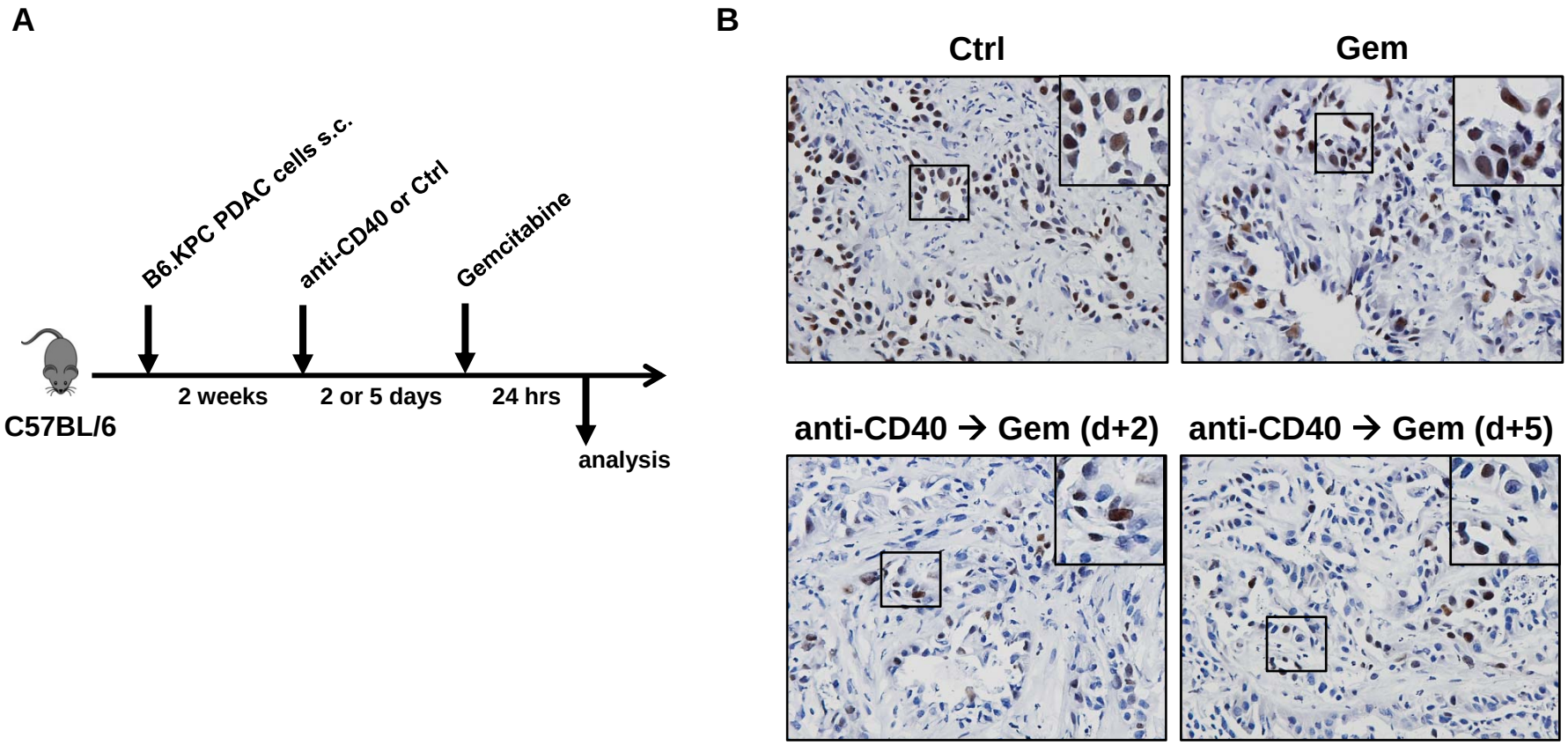

Supplemental Figure 25. Anti-CD40 treatment improves gemcitabine efficacy *in vivo*. a, Schematic showing treatment of mice implanted subcutaneously with a syngeneic PDAC cell line derived from KPC mice. At two weeks after tumor implantation, mice were treated with anti-CD40 antibodies or control (Ctrl) followed by gemcitabine administered two (d+2) or five days (d+5) later. One day post treatment with gemcitabine, tumors were analyzed for the number of $Ki67^+$ cells per hpf. **b,** Representative images showing detection of $Ki67^+$ cells within tumors from indicated treatment groups. Quantification is shown in **Figure 6D**.

Supplemental Figure 26

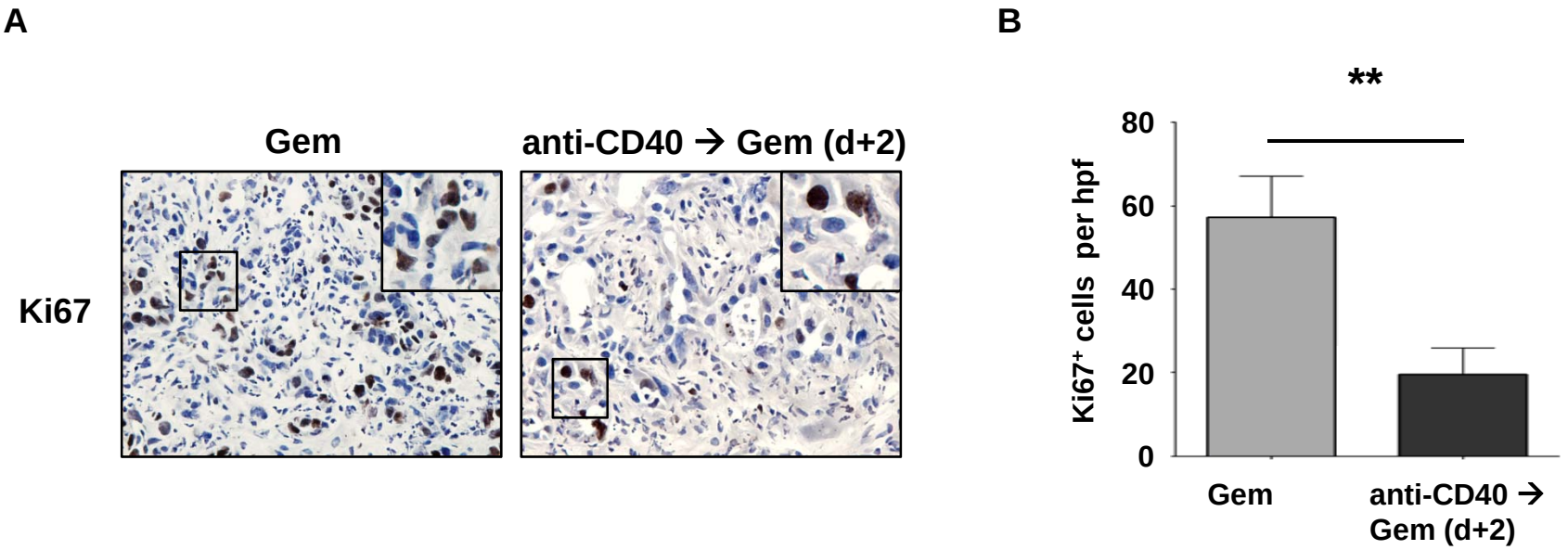

Supplemental Figure 26. Anti-CD40 treatment improves gemcitabine efficacy in KPC tumor-bearing mice. KPC mice were treated with anti-CD40 antibodies or control followed two days later by gemcitabine. One day post treatment with gemcitabine, tumors were analyzed for the number of Ki67$^+$ cells per hpf. **a,** Representative images showing detection of Ki67$^+$ cells within tumors from indicated treatment groups. **b,** Quantification of Ki67$^+$ cells per hpf. *n*=3-4 mice per group, 5 images per mouse. **, *P*<0.01, student's ttest.

Supplemental Figure 27

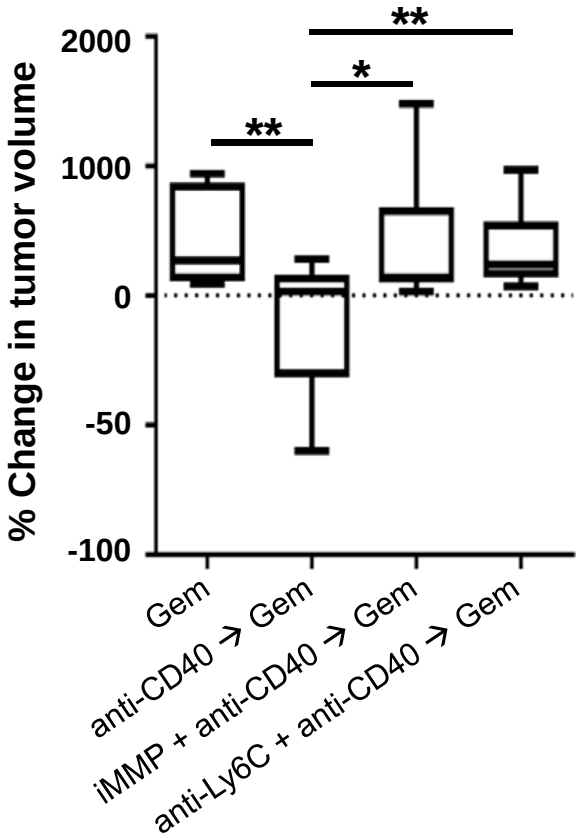

Supplemental Figure 27. Impact of MMPs and Ly6C$^+$ cells on anti-tumor activity induced by gemcitabine administered two days after an agonist CD40 antibody. Mice implanted subcutaneously with a syngeneic PDAC cell line derived from KPC mice were treated with anti-CD40 or control with or without inhibition of MMPs (iMMP, Actinonin) or depletion of Ly6C$^+$ cells. Two days after anti-CD40 treatment, mice received gemcitabine. Shown is the relative change in tumor volume from time of gemcitabine treatment to 6 days later. n=6-13 mice per group. *, P<0.05, **, P<0.01, Student's t test.

Supplemental Figure 28

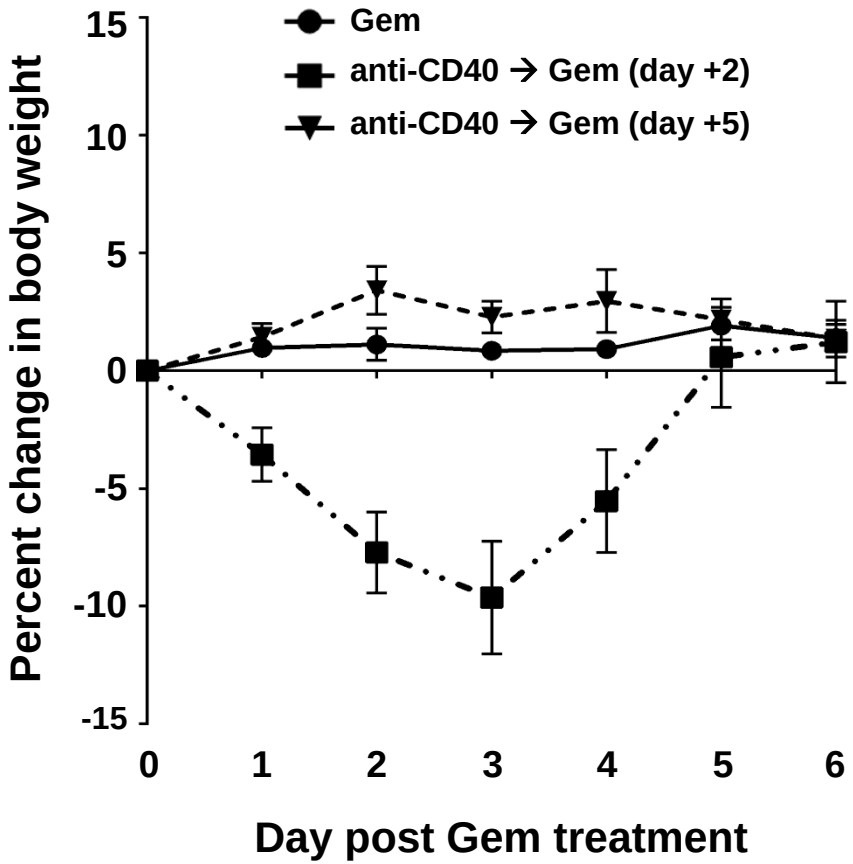

Supplemental Figure 28. Treatment tolerability is dependent on timing of gemcitabine administration after anti-CD40 treatment. Non-tumor-bearing mice were treated with anti-CD40 or control antibodies followed by gemcitabine administered two (day +2) or five days (day +5) later. Shown is the percent change in body weight over time. *n*=4-8 mice per group. Significance testing was performed using one-way Anova with Bonferroni correction for multiple comparisons testing. Error bars represent standard error of the mean, ** $P<0.01$.